Role of surgeon intuition and computer-aided design in Fontan optimization: A computational fluid dynamics simulation study

Yue-Hin Loke, MD,[a] Byeol Kim, BSc,[b] Paige Mass, BSc,[c] Justin D. Opfermann, MS,[c] Narutoshi Hibino, MD, PhD,[d] Axel Krieger, PhD,[b] and Laura Olivieri, MD[a,c]

ABSTRACT

Objective: Customized Fontan designs, generated by computer-aided design (CAD) and optimized by computational fluid dynamics simulations, can lead to novel, patient-specific Fontan conduits unconstrained by off-the-shelf grafts. The relative contributions of both surgical expertise and CAD to Fontan optimization have not been addressed. In this study, we assessed hemodynamic performance of Fontans designed by both surgeon's unconstrained modeling (SUM) and by CAD.

Methods: Ten cardiac magnetic resonance imaging datasets were used to create 3-dimensional (3D) models of Fontans. Baseline computational fluid dynamics simulations assessed Fontan indexed power loss (iPL), hepatic flow distribution, and percentage of conduit surface area with abnormally low wall shear stress for venous flow (<1 dyne/cm^2). Fontans not meeting thresholds were redesigned using 2 methods: SUM (ie, original venous anatomy without the Fontan was 3D printed and sent to surgeon for Fontan redesign with clay modeling) and CAD (ie, the same 3D geometry was sent to engineers for iterative Fontan redesign guided by computational fluid dynamics). Both groups were blinded to each other's results.

Results: Eight Fontans were redesigned by SUM and CAD methods. Both SUM and CAD redesigns met iPL thresholds. SUM had lower iPL, whereas CAD demonstrated balanced hepatic flow distribution and lower wall shear stress percentage. Wall shear stress percentage shared an inverse relationship with iPL, preventing oversized Fontan designs.

Conclusions: Customized Fontan conduits with low iPL can be created by either a surgeon or CAD. CAD can also improve hepatic flow distribution and prevent oversized Fontan designs. Future studies should investigate workflows that combine SUM and CAD to optimize Fontan conduits. (J Thorac Cardiovasc Surg 2020;160:203-12)

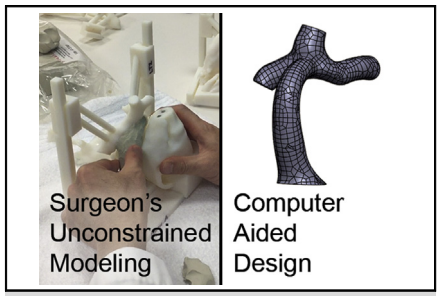

Surgeon's unconstrained modeling (*left*) and computer aided design (*right*) of the Fontan.

CENTRAL MESSAGE

New manufacturing methods for Fontan grafts necessitate new design tools and collaborative approaches. In addition to computer-aided design, surgeons can also directly craft patient-specific Fontan designs with low power loss.

PERSPECTIVE

There is growing interest in the use of customized, patient-specific Fontan designs. Fontan designs can be created by both surgeon and engineering team. Both groups contribute to favorable hemodynamic performance and support an integrative, collaborative approach to optimize graft design and potentially improve surgical result.

See Commentaries on pages 213, 214, and 216.

From the [a]Division of Cardiology and [c]Sheikh Zayed Institute for Pediatric Surgical Innovation, Children's National Hospital, Washington, DC; [b]Department of Mechanical Engineering, University of Maryland, College Park, Md; and [d]Section of Cardiac Surgery, Department of Surgery, University of Chicago/Advocate Children's Hospital, Chicago, Ill.

Supported by National Institutes of Health award numbers R01HL143468 and R21HD090671 as well as University of Maryland supercomputing resources. The content is solely the responsibility of the authors and does not represent the official views of the National Institutes of Health.

Received for publication Sept 26, 2019; revisions received Nov 27, 2019; accepted for publication Dec 13, 2019; available ahead of print Jan 8, 2020.

Address for reprints: Yue-Hin Loke, MD, Division of Cardiology, Children's National Hospital, 111 Michigan Ave, NW, Washington, DC 20010 (E-mail: yloke@childrensnational.org).

0022-5223/$36.00

https://doi.org/10.1016/j.jtcvs.2019.12.068

CONG

Abbreviations and Acronyms

%WSS = percentage of Fontan area with below-physiologic wall shear stress for venous flow
3D = 3 dimensional
AVM = arteriovenous malformation
CAD = computer-aided design
CFD = computational fluid dynamics
CMR = cardiac magnetic resonance
EX = extracardiac
HFD = hepatic flow distribution
iPL = indexed power loss
IVC = inferior vena cava
LPA = left pulmonary artery
LT = lateral tunnel
RPA = right pulmonary artery
SCPC = superior cavopulmonary connection
STL = stereolithography
SUM = surgeon's unconstrained modeling
SVC = superior vena cava

Scanning this QR code will take you to the article title page to access supplementary information.

In the era of personalized health care,[1] significant attention is placed on optimizing the Fontan procedure. Once described as the final stage in single-ventricle palliation,[2] the Fontan operation has suboptimal long-term outcomes, including heart failure and protein losing enteropathy.[3] Fontan patients also demonstrate decreased exercise tolerance,[4] pulmonary arteriovenous malformations (AVM),[5,6] and increased risk for venous thrombosis despite anticoagulation therapy.[7] In response to these known issues, the Fontan operation has undergone several surgical modifications, more recently a bifurcated Y-graft design to specifically improve hepatic flow distribution (HFD) and prevent pulmonary AVM formation.[8] However, the current era of Fontan design remains constrained by off-the-shelf grafts; for example, the Y-graft relies on polytetrafluoroethylene grafts with constraints in vessel diameter.[8,9]

With recent developments in 3-dimensional (3D) technologies such as printed tissue-engineered vascular grafts,[10] there is growing interest in developing customized Fontan graft designs. We have previously demonstrated an integrated approach to create customized, patient-specific Fontan conduits.[11] This approach included image segmentation, computer-aided designs (CAD), modifications guided by computational fluid dynamics (CFD) simulations and electrospinning to create customized Fontan conduits. CFD has been important in predicting the hemodynamic performance of the redesigns.

Several parameters have been identified in the quest to optimize Fontan conduit geometry: lower indexed power loss (iPL), which correlates with improved exercise capacity,[12] and normal HFD to prevent formation of pulmonary AVMs.[13] Of note, there has been no established CFD parameter that prevents oversizing of the Fontan conduit, which contributes to thrombosis and neointimal hyperplasia in the Fontan geometry.[9] Furthermore, most studies investigating Fontan design optimization utilize CAD programs that are not truly unconstrained and free-form as completely intended by the surgeon. Thus, in the next generation of bespoke surgery,[9] a surgeons' role in optimizing Fontan hemodynamic performances has not been clarified.

The objective of this study was to assess the design of Fontan conduits created by surgeon's unconstrained modeling (SUM) as well as the dominant hemodynamic features of Fontan conduits created by SUM and CAD. With SUM, we present a novel method where a 3D model is freely clay sculptured by the surgeon (Figure 1 and Video 1) and then 3D scanned for CFD. We also present a novel CFD criterion that prevents oversizing of Fontan designs. We hypothesize that SUM Fontan conduits can optimize iPL, whereas other hemodynamic parameters may benefit from CAD informed by CFD simulation.

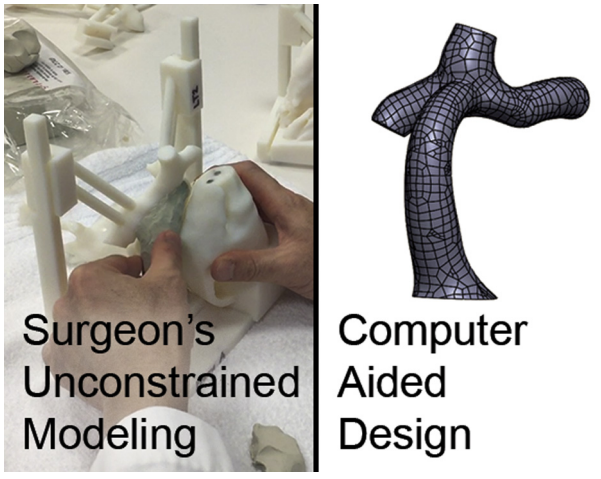

FIGURE 1. Surgeon's unconstrained modeling (SUM) and computer-aided design (CAD) of the Fontan conduit. The novel technique of SUM incorporates clay sculpting to directly craft unconstrained Fontan designs as intended by the surgeon. In comparison, CAD relies on engineers and software to create Fontan conduit designs that are optimized based on computational fluid dynamic parameters.

VIDEO 1. Surgeon's unconstrained modeling (SUM). The novel technique of SUM incorporates clay sculpting to directly hand craft unconstrained Fontan designs as intended by the surgeon. The cardiac surgeon (NH) hand sculpted with a clay representation of the Fontan graft that connected the inferior vena cava into the superior cavopulmonary connection. Afterward, modular components were removed and the SUM Fontan was scanned with Artec Eva Lite (Artec 3D, Luxembourg) into a 3-dimensional digital format. Video available at: https://www.jtcvs.org/article/S0022-5223(20)30050-7/fulltext.

METHODS

3D Modeling of Original Fontan Conduits

This study was approved by the institutional review boards of all participating institutions. Cardiovascular magnetic resonance imaging datasets from 10 Fontan patients (Table 1) were anonymized and exported in Digital Imaging and Communications in Medicine (DICOM) format. Cardiovascular magnetic resonance imaging data included contrast-enhanced, subtracted magnetic resonance angiography and phase contrast velocity flow cines in the cavae (ie, superior vena cava [SVC] and inferior vena cava [IVC]) and the pulmonary arteries (ie, right pulmonary artery [RPA] and left pulmonary artery [LPA]).

Magnetic resonance angiography consisted of a late-phase, nongated, breath-held acquisition with pixel size ~1.4 × 1.4 mm. Using commercially available image segmentation software (Mimics; Materialise, Leuven, Belgium), a 3D digital model of the original Fontan conduit was reconstructed from the blood pool, including the SVC, IVC, RPA, and LPA. The 3D model was then exported in stereolithography (STL) file format, smoothed and hollowed.

CFD Simulation

CFD simulation methodology was the same as detailed in our previous studies.[11,14] The commercial software Ansys Fluent (Ansys Inc, Canonsburg, Pa) was used for CFD simulation. Time-averaged IVC and SVC flow rates were derived from phase velocity data and prescribed as inlet boundary conditions to the CFD simulations. For the outlet boundary conditions, time-averaged RPA and LPA flow rates were prescribed by the product of outlet flow split (RPA:LPA flow) with total venous flow (summation of SVC and IVC flow rate). Other solver parameters are listed in Appendix E1.

Hemodynamic Parameters

The hemodynamic performance of the Fontan conduit and optimization goals were defined by 3 parameters: iPL across the Fontan, HFD, and percentage of Fontan surface area with below-physiologic wall shear stress for venous flow (%WSS), a novel surrogate parameter to prevent Fontan conduit oversizing.

iPL. iPL calculation is based on the methodology of Khiabani and colleagues.[12] iPL is a dimensionless resistive index that correlates with exercise capacity.[12,15] The use of iPL is a form of dimensional analysis that accounts for varying systemic venous flows among Fontan patients. The absolute power loss (P_{loss}) is measured as the difference between the total hemodynamic energy at the inlets and the total hemodynamic energy at the outlets:

$$P_{loss} = \sum_{SVC,IVC} Q\left(\overline{p} + \frac{1}{2}\rho \cdot \overline{u}^2\right) - \sum_{RPA,LPA} Q\left(\overline{p} + \frac{1}{2}\rho \cdot \overline{u}^2\right)$$

where $\overline{p}$ is the static pressure, ρ is density, Q is flow, and $\overline{u}$ is velocity vector. To account for variability in flow rates and patient size, absolute power loss is then indexed against cardiac output and body surface area:

$$\text{iPL} = \frac{P_{loss}}{\rho Q_S^3 / BSA^2}$$

where P_{loss} is the power loss value from equation 1, Q_s is systemic venous flow, and BSA is body surface area. The denominator has the same dimensions as power (Watts or $kg \cdot m^2/sec^3$); thus, indexed power loss is expressed as a dimensionless unit.

TABLE 1. Details of Fontan patients included in study

Patient*	Fontan type	Cardiac anatomy	Other anatomic considerations
EX1	Extracardiac	Hypoplastic left heart syndrome	
EX2	Extracardiac	Hypoplastic left heart syndrome	LPA stenosis
D-EX3	Extracardiac	Unbalanced atrioventricular canal	Dextrocardia, bilateral SVC
D-EX4	Extracardiac	Unbalanced atrioventricular canal	Dextrocardia, apicocaval juxtaposition, left-sided SCPC
L1	Lateral tunnel	L-transposition of great vessels, remote ventricular septal defect	
LT2	Lateral tunnel	Double-inlet left ventricle, pulmonary atresia	
LT3	Lateral tunnel	Double-outlet right ventricle, remote ventricular septal defect	
LT4	Lateral tunnel	Tricuspid atresia	
LT5	Lateral tunnel	Tricuspid atresia	Bilateral SVC, LPA stenosis
AP1	Atriopulmonary	Double-inlet left ventricle	Fontan conversion

Cardiac magnetic resonance data were retrospectively collected and processed from this cohort in our study. *The patient cohort consisted of 4 extracardiac type Fontans (coded as EX; D-EX when there was also dextrocardia), 5 lateral tunnel type Fontans (coded as LT) and 1 atriopulmonary type Fontan (coded as AP). Two patients had dextrocardia, in 1 of these patients there was apicocaval juxtaposition. Two patients had bilateral superior vena cava (SVC), 1 patient had a left-sided superior cavopulmonary connection (SCPC). In 2 patients, significant stenosis was noted across the left pulmonary artery (LPA).

HFD. HFD was defined as the ratio of blood from the IVC to the LPA and RPA, respectively. The HFD was evaluated through particle tracking. A specified number of particles (N_{tot}) were seeded uniformly at the IVC inlet. N_{tot} was determined by evenly spacing the particles across the IVC, with a 0.1 mm marker size and 1 mm spacing factor. The number of particles passing through the RPA and LPA outlets (N_{RPA} and N_{LPA}, respectively) was calculated at the end of the simulation using the velocity field over the last 1000 time steps and averaged. The HFD was calculated as follows:

$$HFD_{LPA} = \frac{N_{LPA}}{N_{tot}}$$

$$HFD_{RPA} = \frac{N_{RPA}}{N_{tot}}$$

%WSS to prevent oversizing. Oversized vessels (relative to flow) will have low WSS which can lead to neointimal hyperplasia and thrombosis.[16,17] Previous CFD-based observations on Fontan Y-graft designs have demonstrated thrombosis in graft limbs with low flow and low WSS.[8,18] The physiologic range of WSS in large veins is 1 to 10 dynes/cm^2 (0.1-1 Pascals).[19] Thus, luminal surface areas with WSS <1 dyne/cm^2 ($Area_{lowWSS}$) were considered below physiologic. The areas of low WSS were quantified as a percentage of the total surface area of the Fontan model ($Area_{Fontan}$), creating the novel parameter % WSS:

$$\%WSS = \frac{Area_{lowWSS}}{Area_{Fontan}}$$

%WSS was calculated from the CFD simulation. A MATLAB script was written to exclude the superior cavopulmonary connection (SCPC) geometry from %WSS calculation, to selectively evaluate the modifiable component of the geometry.

CFD Thresholds for Conduit Optimization

Fontan models with hemodynamic parameters beyond thresholds were selected for conduit optimization. These thresholds include:

- iPL >0.03. This benchmark was based on published literature,[20] particularly a CFD study of hemodynamic parameters in 100 Fontan patients by Haggerty and colleagues.[13] In that cohort, the mean iPL was 0.037 and median iPL was 0.031.
- HFD of RPA:LPA, outside of 40% to 60%/60% to 40% split.
- %WSS >10%.

Methodology for SUM

The original Fontan conduit was removed from the model to create an SCPC model. For lateral tunnel (LT) and atriopulmonary Fontan conduits, a portion of atrial mass was digitally trimmed and smoothed to allow for connection via an extracardiac (EX) conduit. The SCPC, along with the rest of the heart (eg, atria, ventricles, great arteries, and pulmonary veins) were then 3D printed and mounted onto a modular scaffold that could be placed in supine or standing position. The SCPC model was sent to an experienced congenital cardiac surgeon (blinded to original CFD results). The surgeon then sculpted by hand his ideal Fontan design onto the SCPC using modeling clay (Figure 2, *A* and *B*). The rest of the heart and thoracic vascular structures remained in place during sculpting, to ensure that the SUM Fontan was anatomically feasible. The surgeon was also provided with a ruler to guide sculpting. Afterward, the rest of the heart was removed, and the SUM Fontan conduit was 3D scanned (Figure 2, *C*) with Artec Eva Lite (Artec 3D, Luxembourg) and exported into STL format. CFD was repeated on the SUM Fontan conduits.

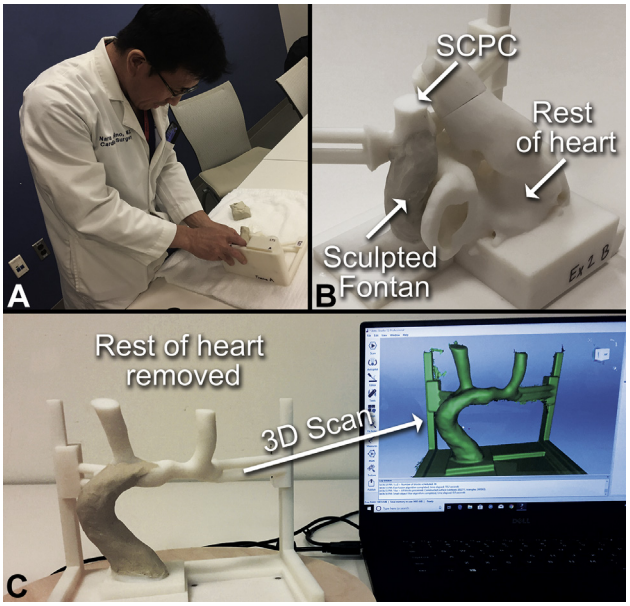

FIGURE 2. Surgeon's unconstrained modeling (SUM). This novel technique incorporates clay sculpting to directly craft unconstrained Fontan designs as intended by the surgeon. A, The designated cardiac surgeon (NH) hand sculpted with a clay representation of the Fontan graft that connected the inferior vena cava into the superior cavopulmonary connection (*SCPC*). The scaffold structure allowed clay sculpting to be performed in either supine or standing position. B, The SCPC and the rest of the heart remained in place during sculpting, to ensure that the sculpted Fontan conduit was anatomically feasible. The SCPC and rest of the heart were held in a modular fashion, such that components could be removed to allow for 3-dimensional (3D) scanning. C, After the modular components were removed, the SUM Fontan conduit was 3D scanned with Artec Eva Lite (Artec 3D, Luxembourg) into a 3D digital format. The SUM Fontan conduit was then evaluated by computational fluid dynamics and compared against computer-aided design Fontan conduits.

Methodology for CAD

CAD Fontan conduits were created over several iterations, in accordance with our previous study (Appendix E1).[11] The same SCPC model and rest of the heart were independently sent to the engineering team as a digital STL format file. The engineering team was responsible for all CFD simulations and not blinded to CFD results, including the CFD results from the original Fontan. Two general strategies were employed to create new designs: flared, tube-shaped conduits or bifurcated conduits. The designs were carefully made against surrounding anatomy, avoiding collision with great arteries and pulmonary veins. All CAD models were created with Solidworks (Dassault Systems, Velizy-Villacoublay, France). The CAD models of the Fontan conduits were modified iteratively: a range of CAD models were CFD-simulated and then compared with parameter thresholds, influential designs were selected, and further modifications made. Modifications included adjusting offset and angle of the Fontan conduit into SCPC to reduce iPL and improve HFD, as well as reducing conduit size to reduce %WSS. After 3 design iterations, the final CAD model with the most optimal hemodynamic performances (lowest iPL and normal range of HFD/%WSS) was selected. The engineering team was blinded to SUM throughout design process and did not receive the SUM Fontan conduits until after final CAD selection. In 2 models (patients EX2 and LT5), significant LPA stenosis was noted; the SCPC was modified by virtually expanding the LPA before SUM and CAD were repeated.

Surgical Feedback for CAD designs

At the end of the study, the surgeon was shown the CFD results of both CAD and SUM Fontan conduits, then given a survey (Appendix E2) to provide feedback on both designs. Survey questions included likelihood of surgically implanting CAD over SUM, technical difficulty of implanting CAD, and aspects of CAD that should be corrected. The answers were provided on a Likert scale.

Statistical Comparison

All statistical analysis was performed with MedCalc version 12.2 (MedCalc Software, Ostend, Belgium). Spearman correlation analysis was used to investigate the relationship between novel parameter %WSS and iPL results across the entire group.

RESULTS

Original Fontan CFD Results

The CFD results of the ten original Fontans are shown in Figure 3. The group consisted of 4 EX Fontans, 5 LT Fontans and 1 atriopulmonary-type Fontan. Of the 10 models, 8 Fontan conduits demonstrated at least 1 hemodynamic parameter outside of thresholds: 3 Fontan conduits with

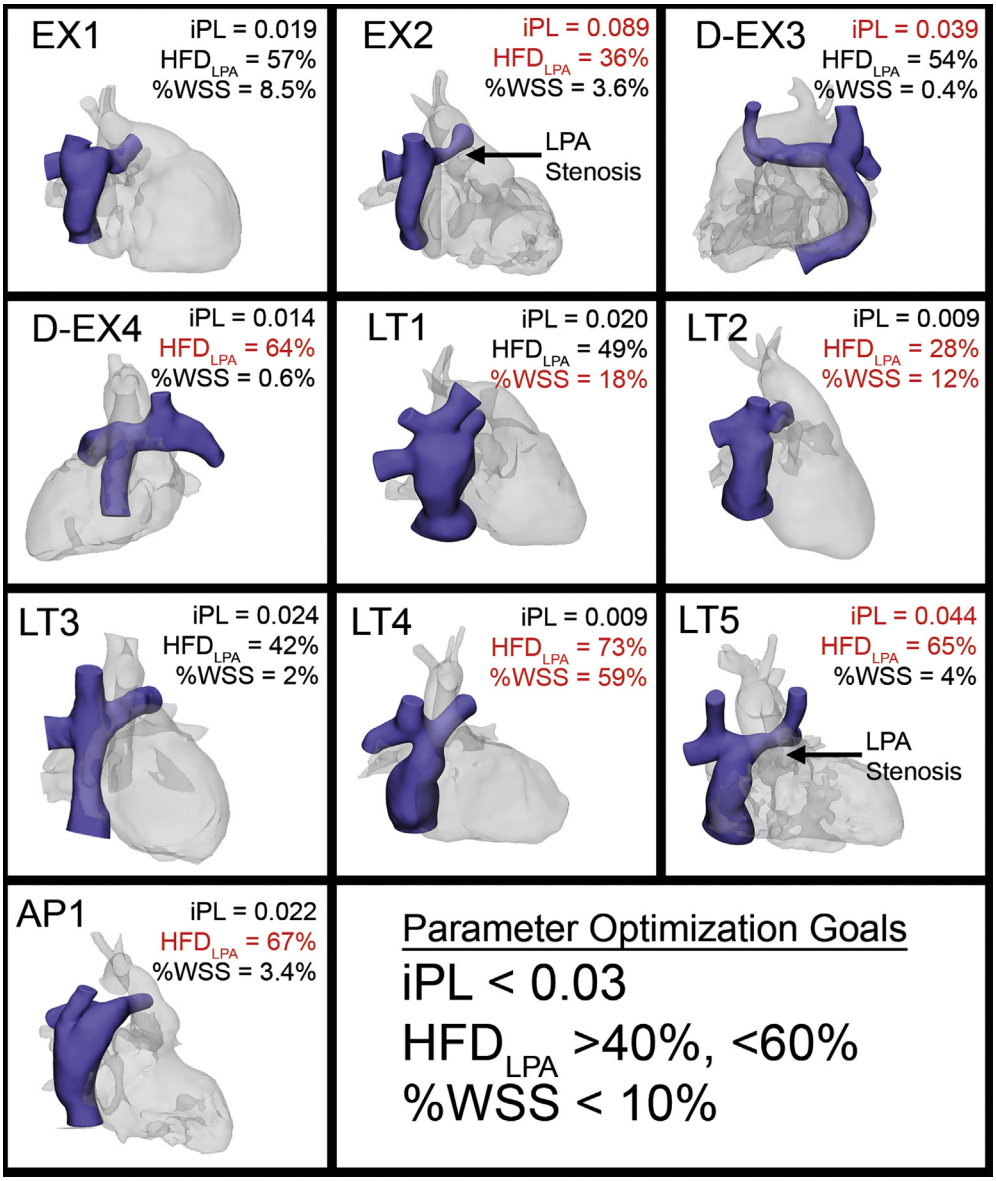

FIGURE 3. Three-dimensional (3D) representation and computational fluid dynamics (CFD) results of original Fontans. A cohort of Fontan patients were retrospectively collected and digitally processed into 3D models for CFD simulation. The cohort consisted of 4 extracardiac-type Fontans (coded as EX or D-EX when there was also dextrocardia), 5 lateral tunnel-type Fontans (coded as *LT*) and 1 atriopulmonary-type Fontan (coded as AP). The CFD results included indexed power loss (*iPL*), hepatic flow distribution of the left pulmonary artery (HFD_{LPA}), and percentage of Fontan surface area with below-physiologic wall shear stress for venous flow (*%WSS*). CFD results in red were considered beyond thresholds. These Fontans were then selected for conduit optimization with parameter optimization goals as listed above. These Fontans underwent either surgeon's unconstrained modeling or computer-aided design.

iPL >0.03, 6 Fontan conduits with suboptimal HFD (ie, beyond 40%-60%/60%-40% split), and 3 Fontan conduits with percent nonphysiologic WSS >10%. The 2 remaining models (EX1 and LT3) had parameters within thresholds and were not included for optimization. For 2 Fontan models (EX2 and LT5), significant narrowing was noted across the LPA that could not be addressed by a Fontan redesign. Because this feature influenced CFD results significantly, the LPA stenosis was virtually stented; that is, expanded to remove this effect from the results between the models.

Redesigned Fontan Conduit CFD Results (SUM and CAD Methods)

Eight sets of SUM and CAD Fontan conduits were created and compared (Figure 4). When compared with the 8 original Fontan conduits, all SUM and CAD Fontan conduits had acceptable iPL <0.03. Of note, the SUM Fontans had lower mean iPL (0.017 ± 0.007) compared with the mean CAD Fontans (0.021 ± 0.004). When compared with the mean of original Fontans (0.031 ± 0.027), both SUM and CAD Fontan conduits trended toward improvement in iPL.

The SUM models had larger range of HFD compared with CAD models. Only 1 of the SUM Fontan conduits had HFD within 40% to 60%/60% to 40% split; whereas all CAD models were within HFD thresholds. For EX2 and LT5, to account for changes in pulmonary flow after virtual LPA enlargement, the simulation tested across a range of RPA:LPA flow splits, a methodology proposed by de Zelicourt and colleagues.[21] In these 2 models, CAD models demonstrated improved balance in HFD compared with SUM models (Figure 5). As illustrated in Figure 6, *A*, HFD was influenced significantly by small changes in conduit offset with the SCPC. For EX2 and the patient with EX and D-EX3, bifurcated grafts were selected because they demonstrated the most stable HFD.

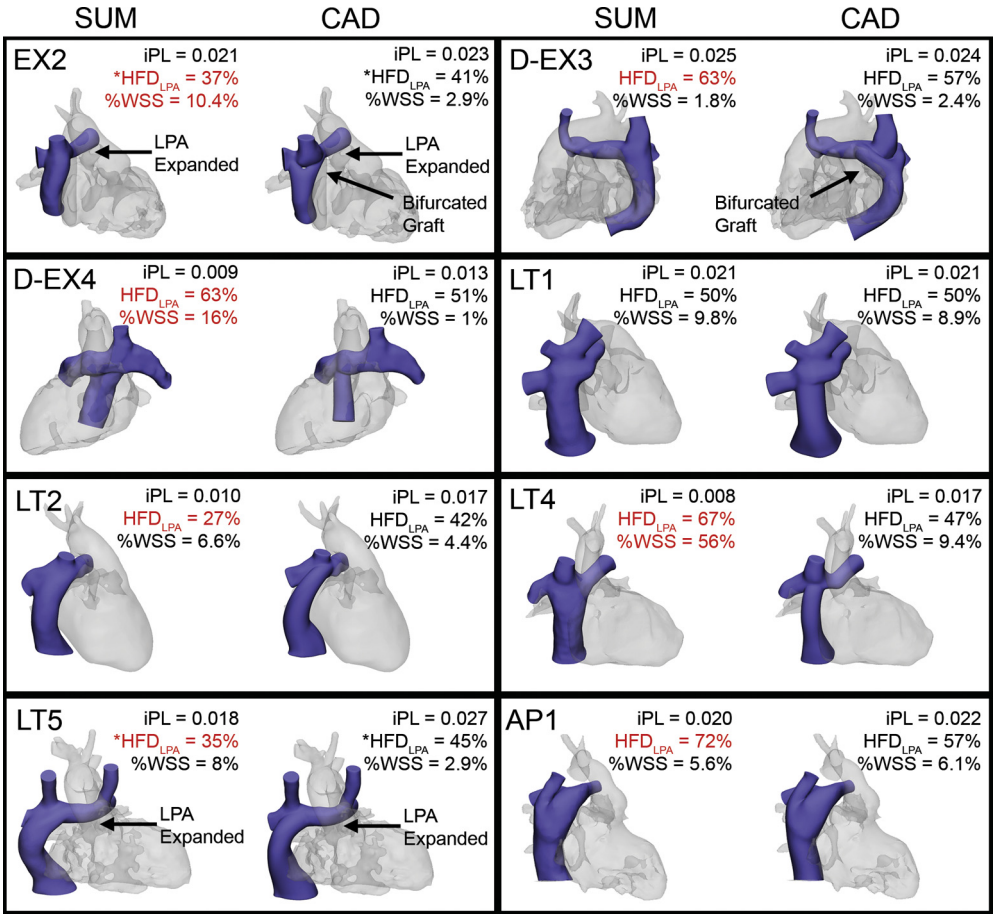

FIGURE 4. Three-dimensional (3D) representation and computational fluid dynamic (CFD) results of surgeon's unconstrained modeling (*SUM*) and computer-aided design (*CAD*). The selected cohort of 8 Fontan models underwent both CAD and SUM, with the resultant new models then re-evaluated by CFD. The CFD results, including indexed power loss (*iPL*), hepatic flow distribution (*HFD*), and Fontan areas with below-physiologic wall shear stress for venous flows (%*WSS*), are labeled for each SUM or CAD result. Results that are labeled in red were considered beyond acceptable threshold parameters. Both SUM and CAD had iPL within thresholds; CAD demonstrated improved HFD and lower %WSS. *LPA*, Left pulmonary artery.

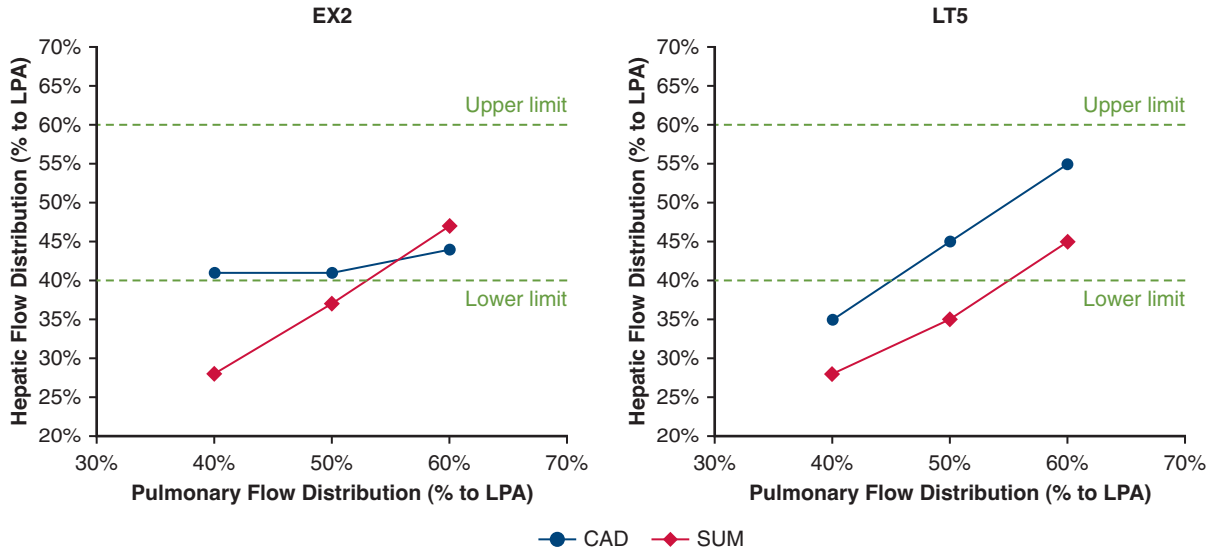

FIGURE 5. Hepatic flow distribution (HFD) relative to pulmonary flow distribution, in surgeon's unconstrained modeling (*SUM*) and computer-aided design (*CAD*) in patient EX2 (extracardiac Fontan in a patient with hypoplastic left heart syndrome and left pulmonary artery [*LPA*] stenosis and patient LT5 (lateral tunnel Fontan with tricuspid atresia, bilateral superior vena cava, and LPA stenosis). In 2 patients within the selected Fontan cohort, significant LPA stenosis was noted that was not modifiable by a new Fontan conduit. A virtual stent was placed across the LPA to reduce power loss. Theoretically, this modification changes the outflow boundary conditions, which potentially affects the HFD results. Thus, in both models created either by SUM or CAD, computational fluid dynamic analysis was performed across a range of pulmonary flow distributions. CAD demonstrated balanced HFD across these ranges.

SUM and CAD models demonstrated similar %WSS when compared with original Fontans. However, 3 of the SUM Fontans had %WSS beyond threshold parameters. Meanwhile, the CAD models had %WSS that were all within threshold parameters. As demonstrated in Figure 6, *B*, there was an inverse relationship appreciated between iPL and %WSS. There was a negative correlation between iPL and %WSS results across the entire group ($r = -0.57$; $P = .003$).

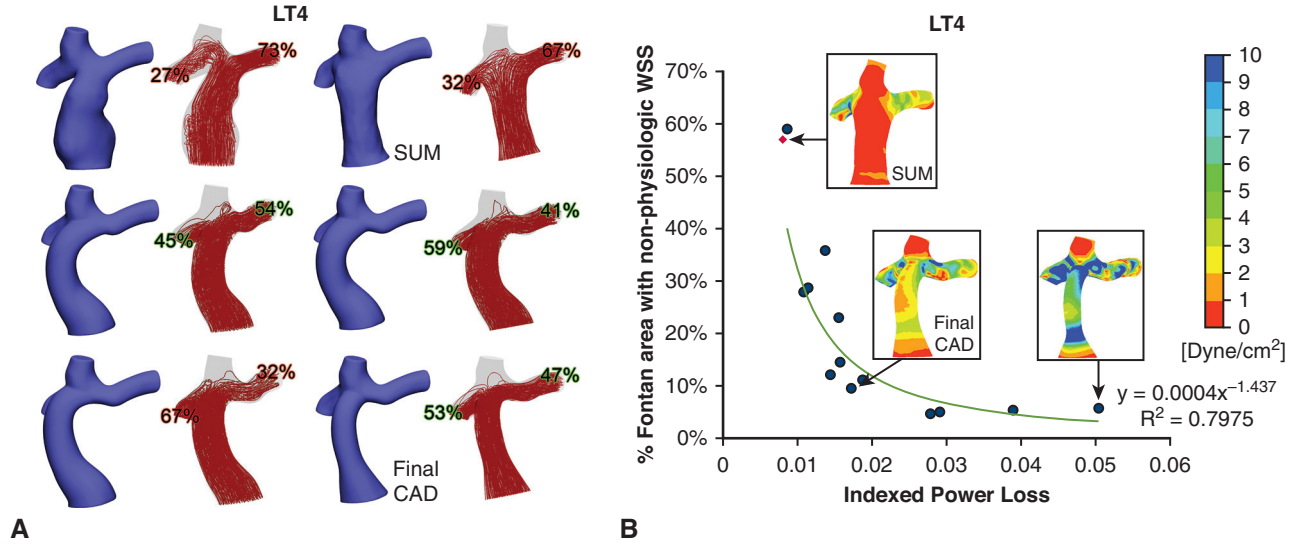

FIGURE 6. Computational fluid dynamics (CFD) results of surgeon's unconstrained modeling (SUM) and all computer-aided design (*CAD*) iterations in patient LT4 (ie, lateral tunnel Fontan patient with tricuspid atresia). To elaborate on the significance of CFD parameters, different iterations of 1 patient are shown. A, The hepatic flow distribution (HFD) iterations across the specific patient LT 4, including SUM, CAD, and final CAD, varied significantly as a result of changes to Fontan flaring, offset, and angulation affect HFD. B, Plot distribution of indexed power loss and lower Fontan areas that had below-physiologic wall shear stress for venous flow (%WSS). There is a negative correlation between both parameters, prohibiting designs that inflated the Fontan conduit (meant to decrease indexed power loss) to disproportionate sizes (which increased percentage of wall shear stress).

Surgical Feedback of CAD Designs

Feedback on all 8 CAD models were provided by the surgeon (Table E1). Out of the 8, 6 were considered by the surgeon to be ''very likely'' used without any significant changes; these models were flared, tube-shaped grafts. Two CAD models (patients EX2 and D-EX3) were considered more complex in surgical implantation, and less likely to be used by the surgeon without significant changes. In both cases, the CADs were bifurcated grafts.

DISCUSSION

To date, this is the first CFD study that investigates the dominant hemodynamic features of both surgeon-led unconstrained designs and computer-based designs of the Fontan conduit. We developed a novel SUM methodology to generate Fontan designs literally crafted by surgical hands and assessed them by CFD. We found that the SUM Fontan conduits were hemodynamically efficient with minimal power loss, although they continued to demonstrate HFD imbalance and larger areas of %WSS. Conversely, some CAD designs were considered complex for surgical implantation and not preferred over SUM/original Fontan designs. This study confirms that a surgeon, independent of material and design constraints, can generate Fontan conduit designs with minimal power loss. However, our results suggest that a surgeon may be challenged by the influence of conduit geometry on WSS and HFD. Thus, this study also clarifies the specific benefit of CAD in terms of balancing HFD and preventing oversized Fontan conduits.

To our knowledge, this is the first known use of clay modeling whilst investigating Fontan conduit hemodynamic parameters. Historically, clay modeling is among the earliest forms of surgical simulation[22] and typically used in medical education.[23] Unlike 3D modeling software or its modern derivatives such as virtual reality, clay modeling provides sensitive haptic feedback for the surgeon.[23] Furthermore, clay modeling allows the surgeon to truly create free-form designs untethered by limitations in CAD geometrical tools (such as lofting or spline functions). For customized Fontans, we believe that SUM can be incorporated into the collaborative approach of graft design: An experienced cardiovascular surgeon can produce an initial clay model that is tested by CFD, with modifications made by CAD before electrospun into a patient-specific optimized design.

Our results are remarkable in that the surgeon's unconstrained designs had low iPL, even when compared with CAD. Hemodynamically inefficient Fontan conduit designs will lead to increased workload on the heart, increased risk for heart failure, and worse clinical outcomes,[24] so minimizing power loss is important. Customized Fontan conduits remove the traditional constraints of surgical materials[9,11] and SUM methodology represents the application of free-form, patient-specific Fontan designs exclusively relying on surgical experience and surgical intuition[25,26] without the aid of CFD or an engineering team. In this study, a surgeon naturally considered the geometrical factors of offset, curving, and flaring, which all contribute to energy reduction.[20] Our results show that surgical intuition makes singular, significant contributions to optimizing Fontan hemodynamic performances, an example of the gut feeling an experienced surgeon uses in predicting postoperative outcomes.[27]

Furthermore, the time involved for SUM was less than CAD (Figure E1). Without surgeon intuition, the engineering team instead relied on a shotgun approach to design, requiring weekly evaluation of CFD results and overall feasibility. This is consistent with other CAD processes requiring >2 weeks of processing to achieve a single optimized design.[28] Meanwhile, the surgeon spent <15 minutes to sculpt each model; thus, SUM could reduce the number of iterations involved. Theoretically, a surgeon could alternatively use dedicated surgical modeling software[29]; however, this method does not include surgeons' haptic feedback and still has geometrical constraints for complex designs.

The CFD-based differences between SUM and CAD demonstrates the additional benefit provided by CAD. As demonstrated in Figure 6, *A*, small adjustments to conduit-SCPC offset and angulation can cause significant changes in HFD, consistent with previous CFD-based observations of the Fontan geometry.[20,30] Incremental changes to offset and angulation (approximately 2 mm and 10°, respectively) resulted in an approximate 5% to 10% change in HFD.

CFD can also identify regions of the Fontan geometry beyond conduit implantation that contribute to hemodynamic inefficiency. As was the case in patients EX2 and LT5, the original CFD simulation determined that LPA stenosis would contribute to significant power loss. In a clinical scenario, virtually expanding the LPA would represent placement of a stent required to reduce iPL. However, the bifurcated grafts generated by CAD still required modifications based on surgical feedback, a statement toward the increased technical complexity of Y-graft Fontan designs.[18] CFD can also identify areas of low flow that contribute to thrombosis and neointimal hyperplasia.[8,17,31,32]

In our study, %WSS is introduced as a novel CFD-based parameter to prevent oversizing of Fontan designs. Studies into the optimal extracardiac Fontan conduit sizes relative to the IVC have shown that oversized Fontan conduits can lead to flow stagnation and thrombosis.[33,34] In other CFD studies, extremely high or low areas of WSS have correlated with areas of thrombosis in vessels.[35,36] WSS is part of the mechanism of thrombosis in Virchow's triad.[16,37] In Virchow's triad, high WSS contributes to platelet activation,

whereas low flow states allow for wall adherence of platelets.[16] For Fontan conduits, the role of WSS has not been validated yet. The only CFD-based study that demonstrated this potential relationship was the validation of the Fontan Y-graft with CFD by Yang and colleagues[8]; one of the Y-graft limbs was noted to significant thrombosis correlating to an area of low WSS.

Nevertheless for CAD, a mechanism such as %WSS is required to prevent oversized Fontan conduits. As illustrated in Figure 6, *B*, %WSS prevented designs that inflated the Fontan conduit to disproportionate sizes (minimizing power loss whilst introducing significant areas of low WSS). Without this parameter, conduit sizes beyond 22 mm would have been developed by CAD. We considered alternative measures, including particle residence time[38] or presence of low velocity fields; however, there are no physiologic standards and neither can isolate the contribution of conduit from the rest of Fontan geometry. Of note, the use of rigid body assumptions in CFD simulation potentially may lead to lower WSS values[39] and thus overestimation of %WSS, although areas of low WSS can still be identified.

In our study, the heart and aortic arch anatomy were included as geometrical constraints. However, the intraoperative environment is different and small variations in surgical placement may occur, potentially limiting the benefits of SUM/CAD. Trusty and colleagues[40] described this effect by comparing HFD results between surgical planning and postoperative anatomy in 12 Fontan patients. In their study, the HFD prediction error was 17% ± 13% and directly correlated with offset error.[40] Thus, prediction of hemodynamic parameters in surgical planning depends on accurate and dynamic representation of in vivo anatomy from 3D modeling.

We only simulated a resting physiologic state and did not consider exercise conditions, which increases venous flow and power loss across the Fontan conduit. At the same time, much of the work from the Cardiovascular Fluid Mechanics Laboratory in Georgia Tech justified our use of iPL, which is flow-independent,[15] predictive of decreased exercise capacity,[12] and directly benchmarked against large cohorts of Fontan patients.[13,20] Other parameters such as power efficiency ($Energy_{Out}/Energy_{In}$) could also be considered; however, the available literature is inadequate to create benchmark parameters.[20]

Our study was limited by small sample size, due to constraints in time (for CAD, 3-4 weeks per case) and resources (for SUM, $400 in 3D printing materials per case). Additionally, our study was limited by method bias, as CAD was directly guided by and iteratively optimized by CFD, leading to favorable CFD results. Thus, this study should not be considered a direct comparison between SUM and CAD. %WSS has not been directly validated outside of observational CFD studies[8,31,41] and the optimization parameter of %WSS <10% was an arbitrary cutoff. Finally, the accuracy of the hemodynamic parameters will be influenced by patient growth, even with tissue-engineered vascular-grafts–based Fontans.[42] Future work will entail CFD simulations of a larger Fontan cohort to clarify %WSS ranges that should be utilized in optimization, longitudinal studies to investigate changes to Fontan geometry after surgical placement, as well as 3D visualization methods that could improve surgical graft placement.

CONCLUSIONS

In the development of customized Fontan designs, we have demonstrated how cardiac surgeons can contribute to Fontan hemodynamics and create efficient Fontan designs based on surgical intuition. CAD can balance HFD and prevent oversizing. Future studies to optimize workflow in patient-specific Fontan design should investigate the combination of both surgical intuition and CAD.

Conflict of Interest Statement

Dr Krieger has a patent pending (Application and Methods of Patient-specific Tissue-engineered Vascular Graft using Electrospinning [US Patent App 62/209,990, August 2016]) and Dr Hibino has a patent issued (No. PCT/US2016/49080). All other authors have nothing to disclose with regard to commercial support.

References

1. Alonso-Betanzos A, Bolón-Canedo V. Big-data analysis, cluster analysis, and machine-learning approaches. *Adv Exp Med Biol*. 2018;1065:607-26.
2. Forbess JM, Cook N, Serraf A, Burke RP, Mayer JE, Jonas RA. An institutional experience with second- and third-stage palliative procedures for hypoplastic left heart syndrome: the impact of the bidirectional cavopulmonary shunt. *J Am Coll Cardiol*. 1997;29:665-70.
3. Atz AM, Zak V, Mahony L, Uzark K, Dagincourt N, Goldberg DJ, et al. Longitudinal outcomes of patients with single ventricle after the Fontan procedure. *J Am Coll Cardiol*. 2017;69:2735-44.
4. Kempny A, Dimopoulos K, Uebing A, Moceri P, Swan L, Gatzoulis MA, et al. Reference values for exercise limitations among adults with congenital heart disease. Relation to activities of daily life—single centre experience and review of published data. *Eur Heart J*. 2012;33:1386-96.
5. Pike NA, Vricella LA, Feinstein JA, Black MD, Reitz BA. Regression of severe pulmonary arteriovenous malformations after Fontan revision and "hepatic factor" rerouting. *Ann Thorac Surg*. 2004;78:697-9.
6. Duncan BW, Desai S. Pulmonary arteriovenous malformations after cavopulmonary anastomosis. *Ann Thorac Surg*. 2003;76:1759-66.
7. Monagle P, Cochrane A, Roberts R, Manlhiot C, Weintraub R, Szechtman B, et al. A multicenter, randomized trial comparing heparin/warfarin and acetylsalicylic acid as primary thromboprophylaxis for 2 years after the Fontan procedure in children. *J Am Coll Cardiol*. 2011;58:645-51.
8. Yang W, Chan FP, Reddy VM, Marsden AL, Feinstein JA. Flow simulations and validation for the first cohort of patients undergoing the Y-graft Fontan procedure. *J Thorac Cardiovasc Surg*. 2015;149:247-55.
9. Chen JM. Bespoke surgery: we're virtually there. *J Thorac Cardiovasc Surg*. 2018;155:1743-4.
10. Fukunishi T, Best CA, Sugiura T, Opfermann J, Ong CS, Shinoka T, et al. Preclinical study of patient-specific cell-free nanofiber tissue-engineered vascular grafts using 3-dimensional printing in a sheep model. *J Thorac Cardiovasc Surg*. 2017;153:924-32.
11. Siallagan D, Loke Y-H, Olivieri L, Opfermann J, Ong CS, de Zélicourt D, et al. Virtual surgical planning, flow simulation, and 3-dimensional electrospinning of

patient-specific grafts to optimize Fontan hemodynamics. *J Thorac Cardiovasc Surg*. 2018;155:1734-42.
12. Khiabani RH, Whitehead KK, Han D, Restrepo M, Tang E, Bethel J, et al. Exercise capacity in single-ventricle patients after Fontan correlates with haemodynamic energy loss in TCPC. *Heart*. 2015;101:139-43.
13. Haggerty CM, Restrepo M, Tang E, de Zélicourt DA, Sundareswaran KS, Mirabella L, et al. Fontan hemodynamics from 100 patient-specific cardiac magnetic resonance studies: a computational fluid dynamics analysis. *J Thorac Cardiovasc Surg*. 2014;148:1481-9.
14. Kim B, Loke Y-H, Stevenson F, Siallagan D, Mass P, Opfermann JD, et al. Virtual cardiac surgical planning through hemodynamics simulation and design optimization of Fontan grafts. *Med Image Comput Comput Assist Interv*. 2019;11768:200-8.
15. Khiabani RH, Whitehead KK, Han D, Restrepo M, Tang E, Bethel J, et al. Does TCPC power loss really affect exercise capacity? *Heart*. 2015;101:575-6.
16. Wolberg AS, Aleman MM, Leiderman K, Machlus KR. Procoagulant activity in hemostasis and thrombosis: Virchow's triad revisited. *Anesth Analg*. 2012;114:275-85.
17. Meyerson SL, Skelly CL, Curi MA, Shakur UM, Vosicky JE, Glagov S, et al. The effects of extremely low shear stress on cellular proliferation and neointimal thickening in the failing bypass graft. *J Vasc Surg*. 2001;34:90-7.
18. Martin MH, Feinstein JA, Chan FP, Marsden AL, Yang W, Reddy VM. Technical feasibility and intermediate outcomes of using a handcrafted, area-preserving, bifurcated Y-graft modification of the Fontan procedure. *J Thorac Cardiovasc Surg*. 2015;149:239-45.e1.
19. Hathcock JJ. Flow effects on coagulation and thrombosis. *Arterioscler Thromb Vasc Biol*. 2006;26:1729-37.
20. Rijnberg FM, Hazekamp MG, Wentzel JJ, de Koning PJH, Westenberg JJM, Jongbloed MRM, et al. Energetics of blood flow in cardiovascular disease: concept and clinical implications of adverse energetics in patients with a Fontan circulation. *Circulation*. 2018;137:2393-407.
21. de Zelicourt D, Kurtcuoglu V. Patient-specific surgical planning, where do we stand? The example of the Fontan procedure. *Ann Biomed Eng*. 2016;44:174-86.
22. Cavalcanti de A Martins A, Martins C. History of liver anatomy: Mesopotamian liver clay models. *HPB*. 2013;15:322-3.
23. Kooloos JGM, Schepens-Franke AN, Bergman EM, Donders RA, Vorstenbosch MA. Anatomical knowledge gain through a clay-modeling exercise compared to live and video observations: clay modeling, live and video observation. *Anat Sci Educ*. 2014;7:420-9.
24. Haggerty CM, Whitehead KK, Bethel J, Fogel MA, Yoganathan AP. Relationship of single ventricle filling and preload to total cavopulmonary connection hemodynamics. *Ann Thorac Surg*. 2015;99:911-7.
25. Duhaylongsod F. Artificial artificial intelligence: surgeon intuition and computers to predict graft patency. *J Thorac Cardiovasc Surg*. 2006;132:466-7.
26. Katlic MR, Coleman J. Surgical intuition. *Ann Surg*. 2018;268:935-7.
27. Markus PM, Martell J, Leister I, Horstmann O, Brinker J, Becker H. Predicting postoperative morbidity by clinical assessment. *Br J Surg*. 2005;92:101-6.
28. Trusty PM, Slesnick TC, Wei ZA, Rossignac J, Kanter KR, Fogel MA, et al. Fontan surgical planning: previous accomplishments, current challenges, and future directions. *J Cardiovasc Transl Res*. 2018;11:133-44.
29. Luffel M, Sati M, Rossignac J, Yoganathan AP, Haggerty CM, Restrepo M, et al. SURGEM: a solid modeling tool for planning and optimizing pediatric heart surgeries. *Comput-Aided Des*. 2016;70:3-12.
30. Tang E, Restrepo M, Haggerty CM, Mirabella L, Bethel J, Whitehead KK, et al. Geometric characterization of patient-specific total cavopulmonary connections and its relationship to hemodynamics. *JACC Cardiovasc Imaging*. 2014;7:215-24.
31. Singer MA, Henshaw WD, Wang SL. Computational modeling of blood flow in the TrapEase inferior vena cava filter. *J Vasc Interv Radiol*. 2009;20:799-805.
32. Gooch KJ, Firstenberg MS, Shrefler BS, Scandling BW. Biomechanics and mechanobiology of saphenous vein grafts. *J Biomech Eng*. 2018;140:020804.
33. Alexi-Meskishvili V, Ovroutski S, Ewert P, Dähnert I, Berger F, Lange PE, et al. Optimal conduit size for extracardiac Fontan operation. *Eur J Cardiothorac Surg*. 2000;18:690-5.
34. Itatani K, Miyaji K, Tomoyasu T, Nakahata Y, Ohara K, Takamoto S, et al. Optimal conduit size of the extracardiac Fontan operation based on energy loss and flow stagnation. *Ann Thorac Surg*. 2009;88:565-73.
35. Buck AKW, Groszek JJ, Colvin DC, Keller SB, Kensinger C, Forbes R, et al. Combined in silico and in vitro approach predicts low wall shear stress regions in a hemofilter that correlate with thrombus formation in vivo. *ASAIO J*. 2018;64:211-7.
36. Kelsey LJ, Powell JT, Norman PE, Miller K, Doyle BJ. A comparison of hemodynamic metrics and intraluminal thrombus burden in a common iliac artery aneurysm. *Int J Numer Methods Biomed Eng*. 2017;33:e2821.
37. Chiu J-J, Chien S. Effects of disturbed flow on vascular endothelium: pathophysiological basis and clinical perspectives. *Physiol Rev*. 2011;91:327-87.
38. Fogel MA, Trusty PM, Nicolson S, Spray T, Gaynor JW, Whitehead KK, et al. Cross-sectional magnetic resonance and modeling comparison from just after fontan to the teen years. *Ann Thorac Surg*. 2020;109:574-82.
39. Long CC, Hsu M-C, Bazilevs Y, Feinstein JA, Marsden AL. Fluid-structure interaction simulations of the Fontan procedure using variable wall properties. *Int J Numer Methods Biomed Eng*. 2012;28:513-27.
40. Trusty PM, Wei ZA, Slesnick TC, Kanter KR, Spray TL, Fogel MA, et al. The first cohort of prospective Fontan surgical planning patients with follow-up data: how accurate is surgical planning? *J Thorac Cardiovasc Surg*. 2019;157:1146-55.
41. Wei W, Pu Y-S, Wang X-K, Jiang A, Zhou R, Li Y, et al. Wall shear stress in portal vein of cirrhotic patients with portal hypertension. *World J Gastroenterol*. 2017;23:3279-86.
42. Sugiura T, Matsumura G, Miyamoto S, Miyachi H, Breuer CK, Shinoka T. Tissue-engineered vascular grafts in children with congenital heart disease: intermediate term follow-up. *Semin Thorac Cardiovasc Surg*. 2018;30:175-9.

Key Words: Fontan operation, computational fluid dynamics, clay modeling, computer-aided design

APPENDIX E1. COMPUTATIONAL FLUID DYNAMICS (CFD) SOLVER PARAMETERS

CFD solver assumptions included laminar flow in the Fontan, rigid body, blood as incompressible fluid, and flat uniform profile at superior vena cava and inferior vena cava. The unsteady Navier-Stokes equations were solved for 3000 time steps. The time step of each iteration was set at 0.001 seconds. A nonuniform triangular meshing with minimal size = 0.7 mm and 5 wall layers was used. Each step was solved within 40 iterations by the SIMPLE numerical solving method. The convergence values were set to 105 for x-, y-, z-velocity and mass conservation residuals. Results were averaged over the last 1000 time steps.

APPENDIX E2. QUESTIONS USED FOR SURGICAL FEEDBACK

Complexity of Design

Please rate the expected complexity in surgical implantation of the computer-aided design (CAD) Fontan geometry compared with surgeon's unconstrained modeling (SUM) and native Fontan.

- Very difficult/not feasible
- Difficult
- No difference
- Easy
- Very easy

Likelihood of Utilizing CAD Geometry

What is the likelihood of utilizing the CAD for the Fontan operation of this specific anatomy?

- Very unlikely (unfeasible)
- Unlikely (+ significant changes needed)
- Possible (+ minor changes)
- Likely (+ minor changes)
- Very likely (no changes needed)

Modifications to CAD Geometry

What are aspects of the CAD that need to be corrected?

- Course of the graft (to adjust for other anatomic structures)
- Size of the graft
- Insertion of the graft into the superior cavopulmonary anastomosis
- Bifurcation of the graft
- Other

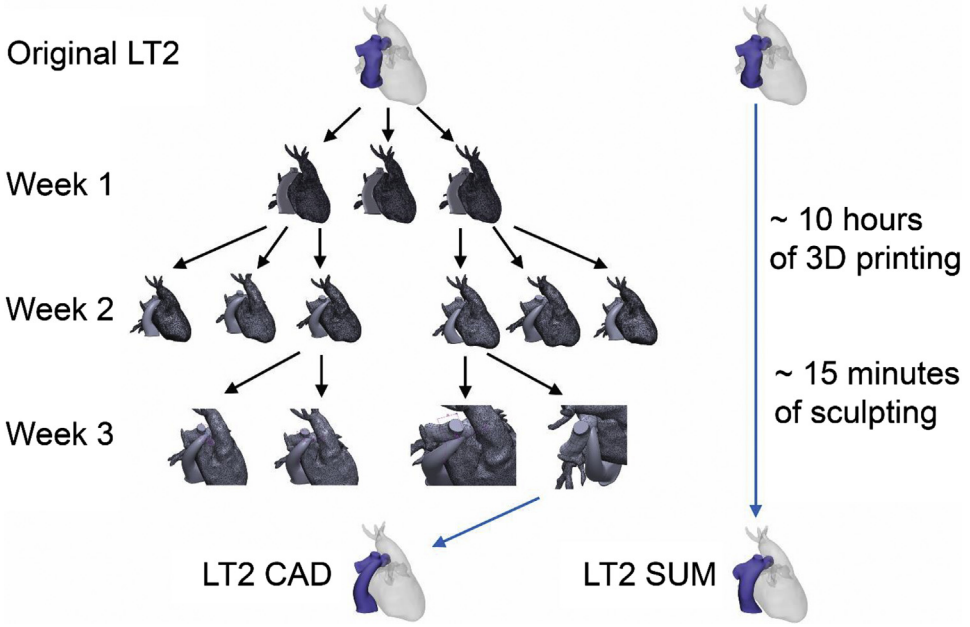

FIGURE E1. Comparison of the process between surgeon's unconstrained modeling (*SUM*) and computer-aided design (*CAD*) in creation of new Fontan conduits. Patient LT2 is demonstrated in this example. The engineering team relied on a shotgun approach to design, requiring weekly meetings to evaluate computational fluid dynamics results and review overall feasibility. Meanwhile, the surgeon spent <15 minutes to sculpt each model as opposed to CAD.

TABLE E1. Surgical feedback on Fontan geometries made by computer-aided design (CAD)

Patient*	Please rate the expected complexity in surgical implantation of CAD, compared with SUM and native Fontan	What is the likelihood of utilizing the CAD for the Fontan operation of this specific geometry?	What are aspects of the CAD that need to be corrected?
EX2	Difficult	Unlikely (+ significant changes needed)	Bifurcation of the graft
D-EX3	Difficult	Unlikely (+ significant changes needed)	Bifurcation of the graft
D-EX4	Difficult	Very likely (no changes needed)	Course of the graft (to adjust for other anatomic structures)
LT1	Very easy	Very likely (no changes needed)	
LT2	Very easy	Very likely (no changes needed)	
LT4	Very easy	Very likely (no changes needed)	
LT5	Difficult	Very likely (no changes needed)	Insertion site of the graft into the superior cavopulmonary anastomosis
AP1	Easy	Very likely (no changes needed)	Insertion site of the graft into the superior cavopulmonary anastomosis

CAD, Computer-aided design; *SUM*, surgeon's unconstrained modeling. *The patient cohort consisted of 4 extracardiac type Fontans (coded as EX; D-EX when there was also dextrocardia), 5 lateral tunnel type Fontans (coded as LT), and 1 atriopulmonary type Fontan (coded as AP). EX1 and LT3 were not included in the process because all their hemodynamic parameters were already within optimization thresholds.